Int. J. Heat Mass Transfer. Vol. 13, pp. 503–516. Pergamon Press 1970. Printed in Great Britain

POOL BOILING FROM LARGE ARRAYS OF ARTIFICIAL NUCLEATION SITES

Y. HELED, J. RICKLIS* and ALUF ORELL

Department of Chemical Engineering, Israel Institute of Technology, Haifa, Israel

(*Received* 19 *June* 1969 *and in revised form* 21 *August* 1969)

Abstract — Pool boiling heat transfer from large and controlled arrays of artificial nucleation sites was studied experimentally. Organic liquids were boiled from artificial sites of uniform size, shape and spacing, drilled in superfinished horizontal surfaces at site densities of 8 and 16 per cm^2. The results confirm the existence of two heat transfer regimes which are characteristic of boiling from a constant number of sites [2]. Appropriate correlations, based on a physical model, were developed for predicting the heat transfer rate in the two regimes over a wide range of site densities and Prandtl numbers. A heat transfer mechanism is proposed and discussed.

NOMENCLATURE

a, thermal diffusivity;
A, boiling heat transfer area;
D_b, bubble break-off diameter;
D_z, bubble diameter at the free liquid surface;
f, bubble emission frequency;
g, gravitational acceleration;
Gr, Grashof number;
h, heat transfer coefficient;
k, thermal conductivity;
N, number of nucleation sites;
N/A, number of sites per unit area;
Nu, Nusselt number;
Pr, Prandtl number;
q, heat transfer rate;
q_s, heat transfer rate at the wall;
q/A, heat flux;
Re, Reynolds number;
S, flow cell size;
T_b, bulk liquid temperature;
T_w, wall temperature;
$T_{w,m}$, mean wall temperature;
T_{sat}, saturation temperature;
ΔT_m, mean wall superheat, $T_{w,m} - T_{sat}$;
ΔT_{sup}, bulk liquid superheat, $T_b - T_{sat}$;
u_s, characteristic velocity near the wall, equation (7);
u_t, bubble terminal velocity;
V_b, bubble volume at break-off;
V_z, bubble volume at the free liquid surface;
z, height of liquid above the heating surface.

Greek symbols

α_s, vapor hold-up near the wall;
θ, bubble contact angle;
λ, latent heat;
μ, viscosity;
ν, kinematic viscosity;
ρ, density;
σ, surface tension.

Subscripts

L, liquid;
m, mean value;
tr, transition;
v, vapor.

INTRODUCTION

THE MECHANISM of heat transfer in nucleate pool boiling is an extremely complex one and has not been completely clarified yet. One great difficulty in determining this mechanism lies in the

* Present address: Du Pont Co., Gibbstown, N.J., U.S.A.

interdependence between the hydrodynamic behavior of the two-phase system and the various heat transfer processes that occur during boiling. In addition, severe complications arise from the fact that the nucleation characteristics of commonly available heating surfaces cannot be rigorously controlled and are therefore unpredictable. The nucleation ability of these surfaces determines the density and the surface distribution of the bubble population at any given ΔT, or heat flux, and thus has a marked influence on the hydrodynamic behavior of the boiling system near the heating surface.

The hydrodynamic effect is governed both by the density of the active sites and the rate and mode of vapor emission at these sites. The investigation of the heat transfer mechanism using commercially available surfaces is hampered by the fact that such heat transfer surfaces do not allow an independent and complete control of the active site density and the bubble emission frequency.

The clarification of the nucleate boiling mechanism could be greatly facilitated if the thermal and hydrodynamic effects were to be decoupled and studied individually. An important experimental tool towards this end is a superfinished boiling surface containing a large number of artificial nucleation sites, arranged in a desired geometrical pattern. Here vapor bubbles are formed only at the artificial sites, while the rest of the surface lies inactive. Such surfaces allow a complete control of the density and distribution of the active sites. Consequently, the effect of the rate and mode of vapor generation from a constant number of sites on boiling heat transfer may be studied directly.

The purpose of this investigation was to study the important variables that govern the heat transfer process during nucleate boiling from large and controlled arrays of evenly-spaced active sites of uniform size. In particular the individual and combined contributions of the active site density and vapor emission rate to nucleate boiling heat transfer were to be determined and evaluated.

BACKGROUND

The effect of a sizable number of articial nucleation sites on boiling heat transfer was first studied by Griffith and Wallis [1]. The boiling curve for water, boiling from a paraffin-coated horizontal surface containing 37 evenly-spaced artificial cavities, was established and compared with that for a similar smooth surface free of artificial cavities. The artificially-drilled surface required a smaller superheat to obtain a given heat flux than the smooth surface.

Miyauchi and Yagi [2] extensively studied nucleate boiling of a variety of liquids from cylindrical cavities on a horizontal surface. The cavities were drilled in a controlled geometrical pattern and the artificial site density ranged from 1 to 64 per cm^2. The resulting boiling curves for constant site densities indicated the existence of two distinct heat transfer regimes. In the low heat flux regime, termed "natural convection boiling region", $q/A \sim \Delta T^{1.4}$. In the "forced convection boiling region", operating at relatively high heat fluxes, $q/A \sim \Delta T^{3.3}$. Miyauchi and Yagi suggested that the first regime is governed by natural convection effects while in the second regime forced convection effects are predominant.

Miyauchi and Yagi correlated the heat transfer results in the upper regime for one specific site density by a forced-convection heat transfer equation that does not account for the definite effect of the artificial-site density on the heat transfer coefficient, as shown by their own data.

Such an effect was also observed by Marto *et al.* [3] during boiling of nitrogen from 7 and 13 evenly-spaced artificial cavities. A definite improvement of the heat transfer coefficient with the increase of site density was reported.

Young and Hummel [4] formed irregularly spaced artificial nucleation sites on a metallic strip by spraying it with Teflon. Improved heat transfer coefficients were obtained, compared to boiling from natural surfaces.

Heat transfer data for boiling from a single artificial nucleation site [3, 5–7] as well as from

two or three artificial cavities [5] have also been reported.

APPARATUS AND PROCEDURE

Apparatus

The boiling experiments were performed in the equipment shown schematically in Fig. 1. The apparatus consisted of a heat transfer section, an electrical heating section and a boiling chamber. The heat generated by the electrical heater was transferred through a cylindrical conductor to a flat horizontal boiling heat transfer surface.

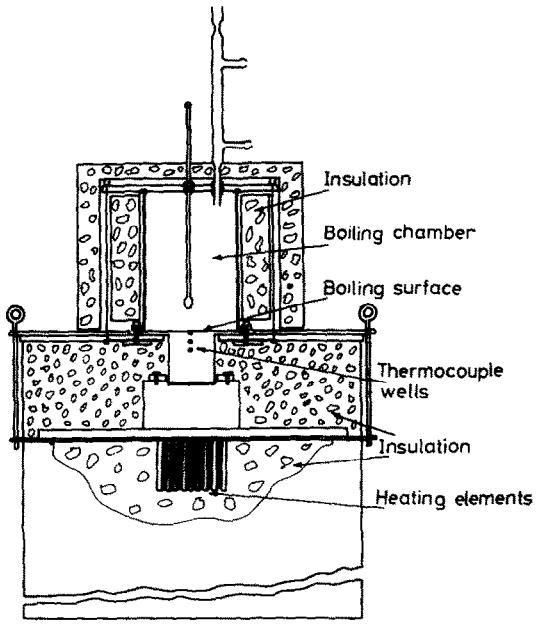

FIG. 1. Experimental apparatus.

The heat transfer section consisted of a brass cylinder 2 in. dia. and 2 in. high. The upper face of the cylinder extended into a flat circular horizontal fin $\frac{1}{16}$ in. thick and $4\frac{1}{4}$ in. o.d. The fin was made an integral part of the cylinder by machining the entire heat transfer section from a single block. Good contact with the heater was assured by embedding the lower end of the cylinder in molten tin, contained in the recessed upper face of the heater.

Seven 30 gage copper–constantan thermocouples were inserted in the conducting section to evaluate the necessary heat transfer data. Three thermocouples, inserted through vertical wells up to a distance of 0·008 in. below the surface, measured the boiling surface temperature. The remaining thermocouples were used to compute the total heat transferred to the liquid through the boiling and fin areas and through the fin alone.

The heater consisted of a circular brass block, with ten square $2\frac{9}{16}$ in. fins extending from its lower part. Nine Nichrome heating elements, encased in mica sheets, were inserted into the slots between the fins. The heater was supported in the center of an asbestos box and was thermally insulated with glass wool.

A 220 V a.c. source line supplied power to the heater through a variable transformer and a voltage regulator. The heater was capable of supplying 2KW at peak performance.

The boiling chamber was a $3\frac{3}{4}$ in. i.d. glass pipe 6 in. long. It was capped by a nickel-plated brass plate, secured by 3 tension wires. The top and bottom sides of the glass pipe were sealed by a silicone rubber gasket and a Neoprene O-ring, respectively. Two reflux condensers returned the condensed vapor back to the boiling chamber. A flow meter and inlet and outlet thermometers were installed in the cooling water line. A calibrated thermometer measured the boiling liquid temperature $\frac{1}{2}$ in. above the heat transfer surface. The chamber was insulated with layers of glass wool and a thick pad of rock wool.

Reliable and reproducible heat transfer data for boiling from artificial nucleation sites require virtually complete elimination of all the naturally occuring nucleation sites. Much time and effort were involved in preparing the boiling surface for its role as a controlled nucleation site surface.

The entire upper surface of the heat transfer section was first finished with progressively finer grades of emery cloth on a buffing machine. The surface was then polished with a 3200 mesh diamond compound and electroplated with bright nickel.

Artificial nucleation sites of uniform size, shape and spacing were drilled on the 2 in. o.d. superfinished boiling surface, using miniature drills 0·008 in. o.d. and 0·041 in. long. The location and spacing of the cavities were determined by drawing the desired pattern on a millimetric graph paper and taping it on the surface. In this manner 135 and later 266 even-spaced cylindrical cavities, having a mouth diameter of 0·008 $\pm$ 0·0004 in. and a depth of 0·039 $\pm$ 0·001 in. were formed. The center-to-center spacing of the cavities was controlled within $\pm$0·010 in. The cavity distribution patterns on the heating surface at site densities of 8 and 16 per cm^2 are illustrated in Fig. 2.

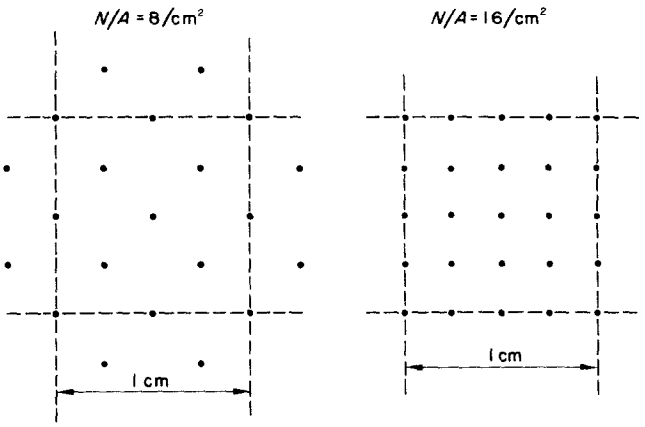

FIG. 2. Distribution patterns of artificial cavities on the heating surface.

Procedure

Prior to each run the heating surface was thoroughly cleaned with benzene and acetone and heated to remove all traces of the solvents. The chamber was then filled with the test liquid up to a constant height of $1\frac{3}{4}$ in. Care was taken to assure that all the cavities became active. The test liquid was degassed by boiling for several hours. By this time the system had reached steady state, as indicated by all the thermocouples.

Up to moderately high heat fluxes, boiling occurred only at the artificial sites. The entire fin region, including the Neoprene O-ring, were inactive. At high heat fluxes, however, natural nucleation sites became active on the boiling surface. Consequently, each series of experiments was terminated when the number of active sites exceeded 10 per cent of the total population of artificial sites. The natural active sites were counted either visually or through the circular scale spots that were deposited around these sites [8].

The heating surface was photographed extensively during boiling at various heat fluxes with a 35 mm Pentax reflex camera, using an electronic flash.

The natural convection experiments were performed after deactivating all the cavities by cooling the test liquid. The upper q/A limit for these runs was set by the initiation of the first bubble at one of the artificial sites.

The total heat transferred to the liquid through the $4\frac{1}{4}$ in. o.d. upper surface was calculated from the readings of the appropriate thermocouples. The measured total heat transfer rate was checked by comparing it with the condenser cooling water heat load. The heat balance was usually closed within $\pm$10 per cent.

The heat transfer rate through the 2 in. dia boiling surface was computed by subtracting the heat transferred by the fin to the liquid by natural convection from the total heat input. The heat rate due to natural convection was calculated by a trial-and-error procedure using a proper fin equation and the appropriate fin thermocouple readings.

The mean wall temperature of the boiling surface was calculated by graphical integration of the surface temperatures over the entire boiling area. The mean wall superheat, $T_{w,m} - T_{sat}$, was used as the mean temperature driving force in this work.

RESULTS

Boiling

Representative boiling heat transfer data for various test liquids are presented graphically as boiling curves in Figs. 3 and 4. Here the *boiling* heat flux is plotted against the mean temperature driving force, ΔT_m, at any given constant site density, N/A.

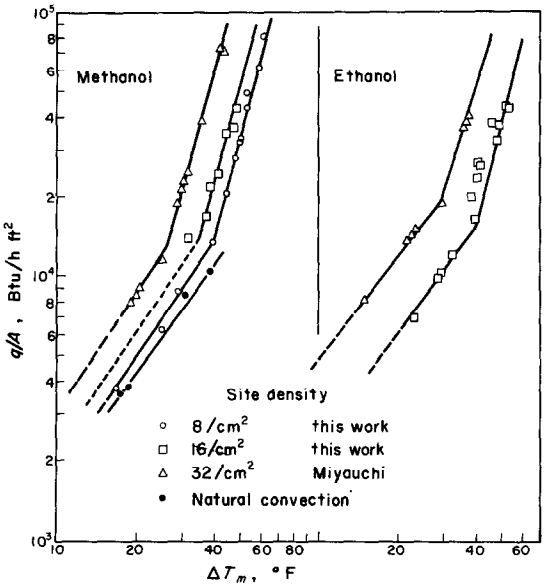

FIG. 4. Boiling curves at constant site densities, methanol and ethanol.

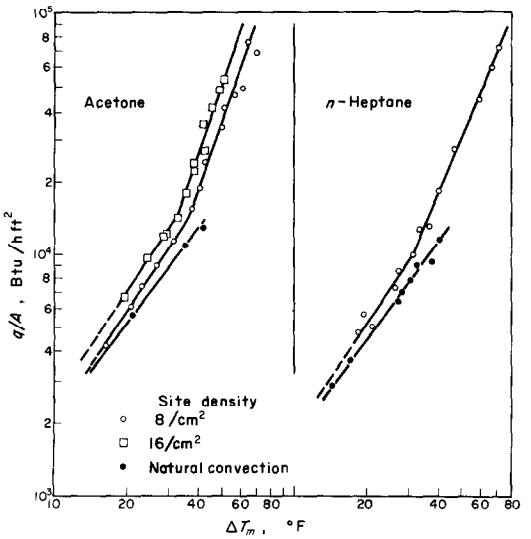

FIG. 3. Boiling curves at constant site densities, acetone and n-heptane.

The boiling curves at constant site densities differ from the classical curves for nucleate boiling from natural active nucleation sites in several respects. First, these curves clearly differentiate between boiling and natural convection. The lowest point in each of these curves corresponds to a boiling heat flux at which all the artificial sites are active. Separate and distinct from the boiling curve is a natural convection curve which relates the heat transferred to the liquid, when the artificial sites are inactive, to ΔT_m. In contrast to artificial sites, the heat transfer data for natural convection, partial and fully developed nucleate boiling from natural sites all lie on a single curve.

Second, the boiling curves in Figs. 3 and 4 indiciate the existence of two distinct boiling heat transfer regimes. The change of the heat flux with ΔT_m up to the maximum value of 20 000 Btu/h ft^2 is quite moderate and the average slope of the boiling curve is not markedly different from that of the natural convection curve. Consequently, the lower portion of the boiling curve has been termed the "low heat flux region". Beyond a narrow transition region

the boiling curve rises rather sharply and characterizes the "high heat flux region".

The existence of two different heat transfer regions where transition from one region to the other occurs within a narrow heat flux range is characteristic of boiling from a constant number of nucleation sites only. Similar behavior has also been observed by Miyauchi and Yagi [2].

Third, the boiling curves for artificial sites are in a sense complete since they indicate the effect of the two major variables on the heat flux, namely ΔT_m and the active site density. Boiling curves for naturally occurring nucleation sites, although in common usage and convenient, do not display the effect of the active site number and spacing on the heat transfer rate directly. As these variables are by no means easy to measure, their effect is usually reported in terms of a polishing paper grade or an r.m.s. surface roughness. The nucleation ability of artificial heat transfer surfaces, on the other hand, is known and controlled and can be represented by a single variable—the active site density. Thus the interrelation between q/A, N/A and ΔT_m for boiling from artificial sites is fully displayed by a boiling curve.

Figures 3 and 4 show that the boiling heat transfer from artificial sites can be improved by increasing either ΔT_m, or N/A, or both. At constant site densities, where q/A in the two regimes is solely dependent on ΔT_m, the heat flux increases monotonically with ΔT_m. The heat transfer rate may also be improved by increasing N/A at any given ΔT_m. Thus, boiling from artificial sites has the clear advantage over boiling from natural surfaces since N/A can be kept constant as q/A is varied.

The transition from the low to the high heat flux region at any given site density occurs over a fairly narrow range and may be approximated by a single point. Table 1 lists the conditions at the transition points, obtained by extrapolating the two branches of the boiling curves of this work and [2].

The transition heat fluxes for all the test liquids lie in a relatively narrow range of 10 000–19 000 Btu/h ft^2. The heat flux for any liquid does not seem to be a function of the site density. Note that a sixteen-fold change of the site density for water does not change the transition heat flux materially.

The increase of the site density has, however, a definite effect on the temperature driving force

Table 1. Experimental and predicted heat fluxes at the transition point

Liquid	Site density (cm^{-2})	ΔT_m (°F)	$(q/A)_{exp}$ (Btu/hft^2)	$(q/A)_{pred}$ (Btu/hft^2)	Deviation %
n-Heptane	8	31·5	10000	11400	+11·4
n-Propanol	8	27·0	15500	15700	+1·3
Methanol	8	42·5	13500	14800	+9·6
Methanol	16	32·5	13500*	14800	+9·6
Methanol [2]	32	23·5	13000	14800	+13·8
Acetone	8	38·5	14000	13700	−2·1
Acetone	16	34·0	14300	13700	−4·2
Ethanol	16	37·0	15500	15600	+0·6
Ethanol [2]	32	30·5	18800	15600	−17·0
Water [2]	4	20·0	19900	19800	−0·5
Water [2]	16	15·5	17600	19800	+12·5
Water [2]	32	12·5	19350	19800	+2·3
Water [2]	64	9·0	19350	19800	+2·3
Benzene [2]	32	30·5	17000	15000	−11·8
CCl_4 [2]	32	32·5	12000	10000	−15·8

* Estimated.

at the transition point. As the site density increases for any liquid ΔT_m decreases monotonically.

Natural convection

Typical natural convection data, obtained after deactivating all the artificial cavities, are presented in Figs. 3 and 4. The data fall within the turbulent natural convection region and indeed exhibit the expected $q/A \sim \Delta T^{\frac{4}{3}}$ relationship.

The data were correlated in Fig. 5 where the Nusselt number is plotted against $Gr \times Pr$. The diameter of the heating surface was used as the characteristic length of the system. The temperature driving force appearing in the Grashof number was defined as the difference between the mean surface temperature and the liquid temperature $\frac{1}{2}$ in. above the surface. The resulting equation is

$$Nu = 0{\cdot}61\,(Gr \times Pr)^{\frac{1}{3}}. \qquad (1)$$

A wide variation of the value of the constant of equation (1) for flat horizontal surfaces is reported in the literature, as seen in Table 2. The value found in this work is similar to the one reported by Miyauchi and Yagi [2]. Both are unusually high. It should be noted, however, that the data in these cases were obtained on horizontal surfaces containing a large number of inactive artificial cavities. Similar improvement of the natural convection heat transfer on surfaces containing drilled inactive cavities was also noted by Marto *et al.* [3]. They postulate that the presence of cavities disturbed the thermal boundary layer, leading to higher heat transfer rates.

The wide range of the reported values of the natural convection constant for smooth surfaces may be linked with the flow pattern of the convection currents near the heating surface. Both Denny [5] and Marto *et al.* [3] observed different types of convection patterns in their experimental apparatus. It is thus conceivable that gross convection currents generated by different chamber geometries (thin, confined liquid layers vs. deep, free-surface pools), heating surface locations (submerged vs. confining) and geometries (flat plates vs. finned discs) will affect natural convection heat transfer.

Table 2. Reported values for natural convection constant

Constant	Surface conditions	Investigator
0·14	Smooth	Reilly *et al.* [12]
0·16	Smooth	Jakob [9]
0·273	Smooth	Jakob *et al.* [18]
0·31	Smooth	Zuber [10]
0·32	Smooth	Lippert and Dougal [11]
0·52	Drilled cavities	Miyauchi and Yagi [2]
0·61	Drilled cavities	This work

CORRELATION OF RESULTS

Model

In order to correlate the heat transfer data in the two regimes, consider first the flow field near a heating surface containing a fixed number of sites that are distributed in a given geometrical pattern. The liquid flow is governed by the departure of vapor bubbles from the surface and their rise through the superheated liquid. Schlieren photographs have shown [13, 14] that once the bubbles detach and rise, they cause an updraught of hot liquid that follows in their wake. This updraught is induced by viscous shear between the rising bubbles and the surrounding liquid. The upflow of liquid above the nucleation site leads to the downflow towards the heat transfer surface. The liquid then flows radially towards the nucleation site where

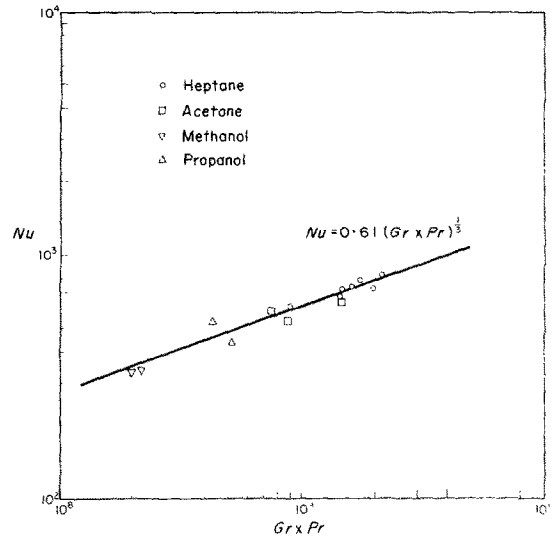

FIG. 5. Natural convection correlation.

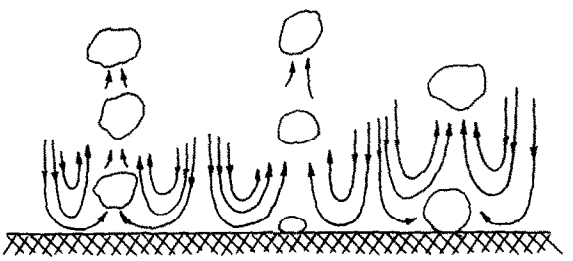

FIG. 6. The flow field near the heat transfer surface.

it rises again. Such a flow pattern is illustrated in Fig. 6.

The lateral space for liquid motion induced by a given site is limited and confined within the boundaries that define a flow cell. Figure 7 describes a cross section of an array of flow cells suggested by the distribution pattern of the artificial cavities on the heating surface. The characteristic size of each recurring cell, S, corresponds to the shortest distance between neighboring cavities.

Heat transfer correlation

The heat transfer data for the two heat transfer regimes were correlated on the basis of the proposed model. The liquid motion near the heat transfer surface in each of the flow cells was approximated by a steady flow over a flat plate having a characteristic dimension of $S/2$.

The data in each regime were fitted with the equation

$$Nu = \text{const.}\, Re^m Pr^n \left(\frac{D_b}{S}\right)^p. \tag{2}$$

The Nusselt number is defined as

$$Nu = \frac{hS}{k_L} \tag{3}$$

where S is directly related to the active site density by

$$S = \left(\frac{N}{A}\right)^{-\frac{1}{2}}. \tag{4}$$

The dimensionless group D_b/S is the ratio of the bubble diameter at break-off and the size of the flow cell. D_b was calculated by the classical Fritz equation

$$D_b = 0{\cdot}021\,\theta \left[\frac{\sigma}{g(\rho_L - \rho_v)}\right]^{\frac{1}{2}}. \tag{5}$$

The Reynolds number is defined as

$$Re = \frac{Su_s\rho_L}{\mu_L} \tag{6}$$

where u_s is the characteristic mean liquid velocity near the heat surface, given by [15] as

$$u_s = \text{const.} \left(\frac{\rho_L - \rho_v}{\rho_L} g\alpha_s \nu_L\right)^{\frac{1}{4}} \tag{7}$$

where α_s is the vapor hold-up near the heat transfer surface. The hold-up can be expressed as

$$\alpha_s = \frac{NV_b f}{Au_t} \tag{8}$$

where V_b is the bubble volume at break-off, f is the bubble emission frequency, and u_t is the bubble terminal velocity. The bubble terminal velocity is given by [16] as

$$u_t = 1{\cdot}53 \left[\frac{g\sigma(\rho_L - \rho_v)}{\rho_L^2}\right]^{\frac{1}{4}}. \tag{9}$$

In the absence of experimental data for bubble frequency and volume the hold-up was evaluated by noting that the numerator in equation (8) is the flow rate of vapor generated at the heat transfer surface by the active sites, or

$$NV_b f = \frac{q_s}{\lambda \rho_v} \tag{10}$$

where q_s is the heat transfer rate due to phase change at the heat transfer surface.

As the volume of the bubble after break-off increases as it rises through the superheated liquid the fraction of the total heat transferred by phase change at the surface is given by

$$\frac{q_s}{q} = \frac{V_b}{V_z} = \left(\frac{D_b}{D_z}\right)^3 \tag{11}$$

where V_z is the bubble volume at the free liquid surface, which is at height z above the heating surface.

The bubble diameter at height, D_z, is given, according to Ruckenstein [17], by

$$D_z^{\frac{7}{4}} - D_b^{\frac{7}{4}} = 0{\cdot}0226 \frac{k_L \Delta T_{sup} z}{\rho_v \lambda a^{\frac{1}{4}}} \tag{12}$$

where ΔT_{sup} is the average superheat of the bulk liquid. The units of the numerical constant are $h^{\frac{1}{4}}/ft^{\frac{1}{4}}$, while D_b and D_z are in feet.

Combining equation (7), (8), (10) and (11) results in

$$u_s = \text{const} \left[\frac{(\rho_L - \rho_v)(q/A) g v_L}{\rho_L \rho_v \lambda u_t} \left(\frac{D_b}{D_z}\right)^3\right]^{\frac{1}{4}}. \tag{13}$$

Fitting the data with equation (2) by a least-squares procedure resulted in the following correlating equations for the low heat flux region

$$Nu = 6{\cdot}83 \times 10^{-2} Re^{1{\cdot}364} Pr^{0{\cdot}949} \left(\frac{D_b}{S}\right)^{0{\cdot}824} \tag{14}$$

and the high heat flux region

$$Nu = 3{\cdot}43 \times 10^{-3} Re^{2{\cdot}023} Pr^{1{\cdot}297} \left(\frac{D_b}{S}\right)^{1{\cdot}408} \tag{15}$$

A comparison of the predicted Nusselt numbers with the experimental values in the two regimes is presented in Figs. 8 and 9. Equations (14) and (15) correlate well both the data of this work and those of Miyauchi and Yagi [2] over a wide range of variables, summarized in Table 3. The maximum deviation of the predicted Nusselt number values in the low flux regime is ± 25 per cent and in the high flux regime is ± 15 per cent.

It is interesting to note that the functional relationship between the heat flux and the major variables in the low flux region is of the form

$$\frac{q}{A} = \text{const.} \left(\frac{N}{A}\right)^{0{\cdot}42} \Delta T_m^{1{\cdot}83}. \tag{16}$$

Zuber [10], using a natural-convection-type correlation for boiling from natural active sites, obtained the approximate relationship

$$\frac{q}{A} \sim \text{const.} \left(\frac{N}{A}\right)^{0{\cdot}33} \Delta T^{1{\cdot}67}. \tag{17}$$

It might be argued, therefore, that these equations are similar and that the data in the low flux region are better correlated by the natural convection approach.

The similarity between the two equations, however, is only superficial. Equation (16) was

Table 3. Range of experimental variables

	Low flux region	High flux region
Heat flux, Btu/h ft^2	3230–19 840	10 050–81 050
Temperature difference, °F	4·3–39·6	12·8–70·7
Site density, cm^{-2}	8–32	8–32
Prandtl number	1·73–9·37	1·73–9·37

obtained by using a forced-convection-type correlation based on the reasoning that the bubble-induced motion inside a flow cell is an important factor in boiling from artificial sites. Such a motion is more pronounced than natural convection flows, induced by density differences. A similar approach was also taken by Ruckenstein [15] and others.

In addition, equation (16) is applicable only when both N/A and ΔT_m may be varied *independently*. Zuber's equation, on the other hand, was obtained by neglecting the natural convection effect compared to the effect of vaporization [10] and applies only to natural surfaces, where new sites are constantly activated as q/A is increased.

The ability of equations (14) and (15) to correlate the data over a wide range of variables substantiates their generalized character. The equations indicate that the heat flux in the two regimes is strongly dependent on the flow cell size. In addition, they show that the liquid velocity near the heat transfer surface, as given by equation (7), is an important variable that governs the heat transfer rate in boiling from artificial sites.

Transition point

In using equations (14) and (15) for prediction of heat transfer coefficients in the two regimes an estimate of the value of the heat flux at the transition point is required. The experimental data in Table 1 show that the heat flux at the transition point is independent of the site density and is practically constant for a given liquid. This suggests that its particular value may be correlated by the physical properties of the boiling liquids. The following empirical correlation was thus developed

$$\left(\frac{q}{A}\right)_{tr} = 0{\cdot}295\,\rho_v\lambda\left(\frac{g\sigma}{\rho_L}\right)^{\frac{1}{4}}. \qquad (18)$$

The predicted heat fluxes at the transition point, shown in Table 1, are in good agreement with the experimental values and the maximum deviation does not exceed 17 per cent. The deviations are reasonable, as most of the experimental transition points were determined by graphical extrapolation and not by design.

DISCUSSION

Nucleate pool boiling from a large array of artificial nucleation sites is characterized by the existence of two heat transfer regimes separated by a narrow transition region. An attempt will be made to postulate a heat transfer mechanism for the two regimes and analyze the experimental results in the light of the proposed mechanism.

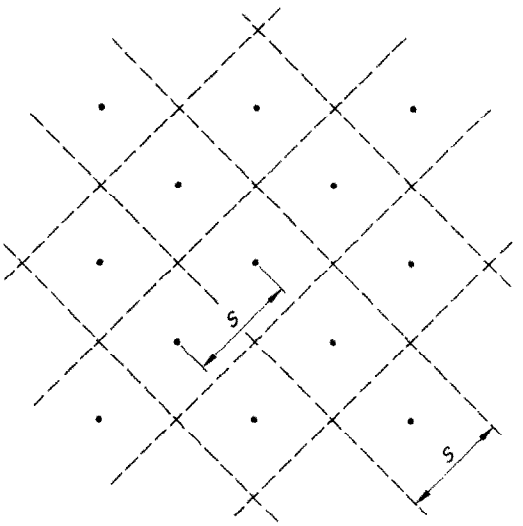

FIG. 7. An array of flow cells at site density of 8/cm^2.

Heat transfer mechanism

The heat transfer process during boiling from a large array of artificial sites is governed by the two-phase flow field close to the heating surface. Of prime importance is the vapor-induced liquid velocity near the surface since it directly determines the heat transfer rate, as indicated by equations (14) and (15). At a constant site density this velocity is solely dependent on the bubble frequency, equations (7) and (8). Consequently, the increase in the heat transfer rate can be entirely attributed to increased bubble frequency if the bubble volume at detachment is assumed constant.

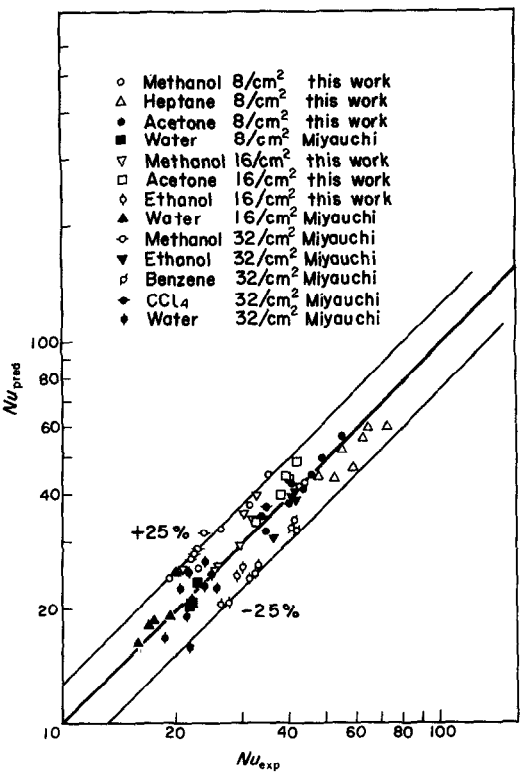

FIG. 8. Comparison of predicted Nusselt numbers with experimental values in the low heat flux region.

It is reasonable to assume that the bubble emission frequency is a function of ΔT. As ΔT increases both the bubble growth period and waiting time become shorter and the frequency increases. As high frequencies are reached, successive bubbles leaving the site would tend to collide and coalesce, finally forming a continuous vapor column. Numerous still photographs taken during this study show that such columns were not present near the heating surface and that individual bubbles formed at the artificial sites.

The existence of two different heat transfer regimes at constant site densities suggests that each regime is characterized by a different mode of bubble emission frequency. It is postulated that in the low flux region the average bubble frequency is a weak function of ΔT as the contribution of bubble generation to the total heat transfer does not change appreciably with ΔT_m.

In the high heat flux region it is assumed that the average bubble frequency is strongly dependent on ΔT. Thus, the marked change in the frequency leads to a sharp increase of the heat transfer rate compared to the moderate rate at the low heat flux regime.

Effect of site density

The boiling heat transfer rate for artificial sites may be changed at any given ΔT_m by simply varying the site density. For example, the heat flux for methanol at ΔT_m of 20°F is increased by 75 per cent as the site density is changed from 8 to 32 per cm^2. As both ΔT_m and bubble frequency remained fixed the improvement in the heat transfer rate results from an enhancement of the liquid velocity due to a decrease in the flow cell size.

It should be noted, however, that the heat transfer rates cannot be increased indefinitely by using heat transfer surfaces containing artificial sites. At high site densities the flow cell size will become comparable to the bubble size at break-off and neighboring bubbles would coalesce laterally while still on the surface. The heating surface would progressively be covered with vapor and the heat transfer rate will eventually reach a maximum value. In addition, the high heat fluxes would activate natural nucleation sites and the idealized behavior of the heating surface will change altogether.

Boiling vs. natural convection

The contribution of bubble generation to the total heat transfer in the low heat flux region does not change appreciably with ΔT_m. In contrast, the contribution of fully developed boiling from natural sites may become appreciable as ΔT increases.

The moderate change with ΔT of the enhancement of the heat transfer over and above the heat transferred by natural convection may be attributed to the weak dependency of bubble

frequency upon the temperature difference. In the limiting case the heat transfer enhancement will become constant as the bubble frequency remains fixed. This is verified by the work of Preckshot and Denny [5] where the average frequency of bubbles emitted from a group of one, two or three artificial sites and the appropriate boiling and natural convection curves were determined. Inspection of their data over the wide temperature range 40–77°F shows that both the contribution of boiling and bubble frequencies remained constant.

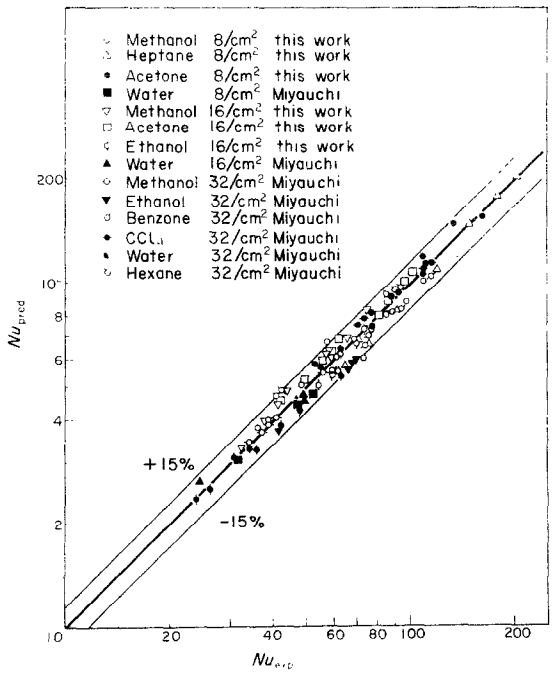

FIG. 9. Comparison of predicted Nusselt numbers with experimental values in the high heat flux region.

The extent of the heat transfer enhancement due to boiling at a constant ΔT_m is determined by the site density, or the flow cell size. As the site density is increased from 8 to 16 and then to 32 per cm^2 the heat flux relative to natural convection, for methanol at 25°F, increases by 17, 47 and 104 per cent respectively. The contribution becomes sizable at high site densities since the liquid velocity in such small flow cells is increased appreciably. Analysis of Miyauchi and Yagi data shows the same trend.

The maximum incremental contribution of boiling from 135 sites to natural convection was found to be 25 per cent. Such an increase of the heat transfer rate is unexpectedly low. It should be borne in mind, however, that the natural convection heat fluxes in presence of a large array of inactive artificial cavities are larger by factors of 2–3 than the fluxes obtained on smooth surfaces.

The extent of heat transfer enhancement in the high flux regime is high and comparable to that for boiling from natural sites, as the slope of the boiling curves in these two cases may be similar. This effect, however, is achieved in two different ways: by high bubble frequencies in boiling from a fixed number of sites and through constant activation of new sites in boiling from natural surfaces.

The transition region

Equation (14) indicates that the relationship between the major parameters in the low heat flux regime is of the general form

$$\frac{q}{A} \sim (\Delta T_m)^a \left(\frac{N}{A}\right)^b. \tag{19}$$

Equation (19) shows that at the transition point, where q/A for any liquid is constant, ΔT_m has to be inversely proportional to N/A, as noted from Table 1.

The reason for the change in the mode of bubble emission at the transition region that affects the liquid velocity near the surface and leads to an improved heat transfer rate at the high flux regime is not yet clear. Miyauchi and Yagi, while attempting to ascribe the existence of the two regimes to natural convection and forced convection effects, respectively, did not give any consideration to the transition region. Further clarification of the postulated change in the mode of bubble emission has yet to await the results of high speed motion photography.

CONCLUSIONS

1. A heat transfer surface containing a controlled number of evenly-spaced active sites is an important research tool for evaluating the individual and combined contributions of two major variables, active site density and bubble emission frequency, to nucleate boiling heat transfer. These variables directly affect the liquid velocity near the heating surface which, in turn, governs the heat transfer process.

2. Nucleate boiling at constant site densities is characterized by two heat transfer regimes, controlled by different vapor generation modes.

3. The individual effects of bubble frequency and site density on boiling heat transfer in each regime may be combined in a correlation that predicts heat transfer coefficients over a wide range of variables.

4. The heat flux at the transition from one regime to the other is independent of the site density and may be predicted with reasonable accuracy.

5. Natural convection heat transfer on a horizontal surface may be markedly affected by the presence of a large number of deactivated artificial sites.

ACKNOWLEDGEMENT

The authors are indebted to Professor S. G. Bankoff of Northwestern University for reviewing the original manuscript and for his helpful comments.

REFERENCES

1. P. Griffith and J. D. Wallis, The role of surface conditions in nucleate boiling, *Chem. Engng Prog. Symp. Ser.* **56**, 49 (1960).
2. T. Miyauchi and S. Yagi, Nucleate boiling heat transfer on horizontal flat surfaces, *Kagaku Kogaku* **25**, 18 (1961).
3. P. J. Marto, J. A. Moulson and M. D. Maynard, Nucleate pool boiling of nitrogen with different surface conditions, *J. Heat Transfer* **90**, 437 (1968).
4. R. K. Young and R. L. Hummel, Improved nucleate boiling heat transfer, *Chem. Engng Prog.* **60**, 53 (1964).
5. G. W. Preckshot and V. E. Denny, Exploration of surface and cavity properties on the nucleate boiling of carbon tetrachloride, *Can. J. Chem. Engng* **45**, 241 (1967).
6. J. E. Benjamin and J. W. Westwater, Bubble growth in nucleate boiling of a binary mixture, *Int. Dev. Heat Transfer*, Part II, pp. 212–218. Am. Soc. Mech. Engrs, New York (1961).
7. E. I. Goltsova, The effect of a single center of vapor formation and the frequency of vapor bubble separation at this center on the wall temperature, *Int. Chem. Engng* **6**, 406 (1966).
8. Y. Heled and Aluf Orell, Characteristics of active nucleation sites in pool boiling, *Int. J. Heat Mass Transfer* **10**, 553 (1967).
9. M. Jakob, *Heat Transfer*, Vol. I, p. 641. John Wiley, New York (1949).
10. N. Zuber, Nucleate boiling. The region of isolated bubbles and the similarity with natural convection, *Int. J. Heat Mass Transfer* **6**, 53 (1963).
11. T. E. Lippert and R. S. Dougal, A study of the temperature profiles measured in the thermal sublayer of water, Freon-113 and methyl alcohol during pool boiling, *J. Heat Transfer* **90**, 347 (1968).
12. I. G. Reilly, C. Tien and M. Adelman, Experimental study of natural convection heat transfer in a non-newtonian fluid. Part II. Horizontal plate, *Can. J. Chem. Engng* **44**, 61 (1966).
13. N. Isshiki and H. Tamaki, Photographic study of boiling heat transfer mechanism, *JSME Bull.* **6**, 505 (1963).
14. R. Séméria, Les echanges thermiques en ebullition nuclée, Publications Scientifiques et Techniques du Ministére de l'Air, No. 147 (1963).
15. E. Ruckenstein, Remarks on nucleate boiling heat transfer from a horizontal surface, *Int. J. Heat Mass Transfer* **9**, 229 (1966).
16. T. Harmathy, Velocity of large drops and bubbles in media of infinite and restricted extent, *A.I.Ch.E. Jl* **6**, 281 (1960).
17. E. Ruckenstein, On heat transfer between vapor bubbles in motion and the boiling liquid from which they are generated, *Chem. Engng Sci.* **10**, 22 (1959).
18. M. Jakob and W. Link, *Heat Transfer*, Vol. I, p. 531. John Wiley, New York (1949).

EBULLITION EN RÉSERVOIR À PARTIR DE GRANDES RANGÉES DE SITES DE NUCLÉATION ARTIFICIELLE

Résumé—Le transport de chaleur dans l'ébullition en réservoir à partir de grandes rangées contrôlées de sites de nucléation artificielle a été étudié expérimentalement. Les liquides organiques ont été mis en ébullition à partir de sites artificiels de taille, de forme et d'espacement uniformes, percés dans des surfaces horizontales de grand fini à des densités de sites de 8 et de 18 par centimètre carré. Les résultats confirment l'existence de deux régimes de transport de chaleur qui sont caractéristiques de l'ébullition à partir d'un

nombre constant de sites (2). Des corrélations appropeiées basées sur un modèle physique, ont été élaborées pour prédire la densité de flux de chaleur dans les deux régimes avec une large gamme de densités de sites et de nombres de Prandtl. Un mécanisme de transport de chaleur est proposé et discuté.

BEHÄLTERSIEDEN ÜBER AUSGEDEHNTEN FLÄCHEN MIT KÜNSTLICHEN SIEDEKEIMEN

Zusammenfassung— Der Wärmeübergang beim Behältersieden an ausgedehnten und definierten Bereichen mit künstlichen Siedekeimen wurde experimentell untersucht. Verwendet wurden organische Flüssigkeiten. Künstliche Siedekeime von gleichmässiger Grösse, Gestalt und Rauminhalt, wurden als Bohrungen in feinpolierten horizontalen Oberflächen mit einer Besetzungsdichte von 8 und 16 pro Quadratzentimeter hergestellt. Die Ergebnisse bestätigen die Existenz zweier Wärmeübergangsgebiete, welche charakteristisch für das Sieden bei einer konstanten Keimzahl sind (2). Geeignete Beziehungen, basierend auf einem physikalischen Modell, wurden entwickelt für die Bestimmung des Wärmestromes in den beiden Gebieten über einen weiten Bereich von Keimstellendichten und Prandtl-Zahlen. Ein Wärmeübertragungsmechanismus wurde vorgeschlagen und diskutiert.

КИПЕНИЕ В БОЛЬШОМ ОБЪЕМЕ В СИСТЕМАХ ИСКУССТВЕННЫХ ЦЕНТРОВ ПАРООБРАЗОВАНИЯ

Аннотация—Экспериментально изучался теплообмен при кипении в большом объеме в крупных и регулируемых системах искусственных центров парообразования. Кипение органических жидкостей происходило на искусственных центрах парообразования одтнакового размера, формы и с одинаковым расстоянием между ними. Искусственные центры парообразования были высверлены на горизонтальных полированных поверхноснях при «плотности» участков от 8 до 16 на квадратный сантиметр. Результаты подтверждают существование двух режимов переноса тепла, характерных для кипения при постоянном числе центров парообразования (2). На основании физической модели разработаны корреляции для расчета скорости тепловых потоков при этих двух режимах и большом диапазоне изменения плотности и числе Прандтля. Предложен и обсуждается механизм переноса тепла.